AIP | The Journal of Chemical Physics

Chirality and hydrogen bonding in molecular crystals for phasematched secondharmonic generation: N(4nitrophenyl)(L)prolinol (NPP)

J. Zyss, J. F. Nicoud, and M. Coquillay

Citation: J. Chem. Phys. **81**, 4160 (1984); doi: 10.1063/1.448134
View online: http://dx.doi.org/10.1063/1.448134
View Table of Contents: http://jcp.aip.org/resource/1/JCPSA6/v81/i9
Published by the American Institute of Physics.

Additional information on J. Chem. Phys.

Journal Homepage: http://jcp.aip.org/
Journal Information: http://jcp.aip.org/about/about_the_journal
Top downloads: http://jcp.aip.org/features/most_downloaded
Information for Authors: http://jcp.aip.org/authors

ADVERTISEMENT

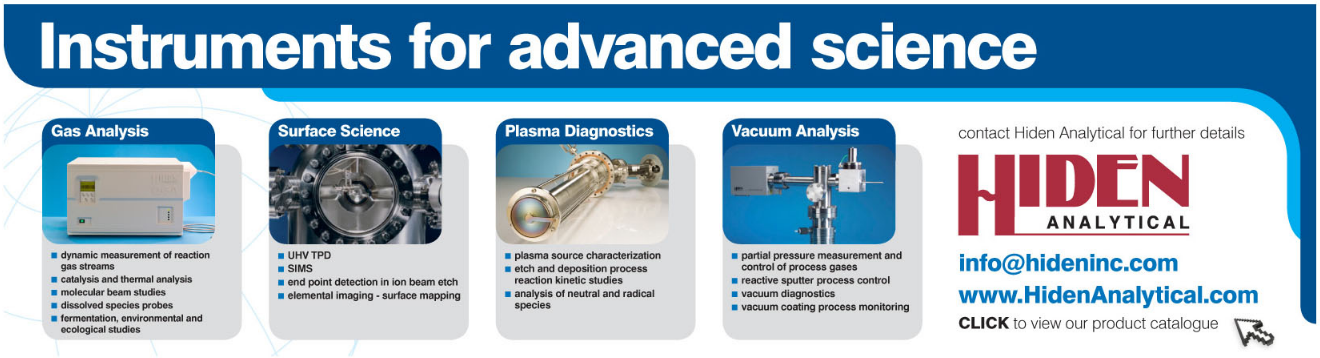

Instruments for advanced science

Gas Analysis
- dynamic measurement of reaction gas streams
- catalysis and thermal analysis
- molecular beam studies
- dissolved species probes
- fermentation, environmental and ecological studies

Surface Science
- UHV TPD
- SIMS
- end point detection in ion beam etch
- elemental imaging - surface mapping

Plasma Diagnostics
- plasma source characterization
- etch and deposition process reaction kinetic studies
- analysis of neutral and radical species

Vacuum Analysis
- partial pressure measurement and control of process gases
- reactive sputter process control
- vacuum diagnostics
- vacuum coating process monitoring

contact Hiden Analytical for further details
HIDEN ANALYTICAL
info@hideninc.com
www.HidenAnalytical.com
CLICK to view our product catalogue

Downloaded 27 Mar 2013 to 129.25.131.235. This article is copyrighted as indicated in the abstract. Reuse of AIP content is subject to the terms at: http://jcp.aip.org/about/rights_and_permissions

Chirality and hydrogen bonding in molecular crystals for phase-matched second-harmonic generation: *N*-(4-nitrophenyl)-(*L*)-prolinol (NPP)

J. Zyss
Laboratoire de Bagneux (La CNRS n° 250), CNET, 196 Rue de Paris, 92220 Bagneux, France
J. F. Nicoud
Laboratoire de Synthèse Asymétrique (La CNRS n° 255), Institut de Chimie Moléculaire, Bât. 420, Université de Paris-Sud, 91405 Orsay, France
M. Coquillay
Laboratoire de Physique, Tour B Centre Pharmaceutique, 92290 Chatenay–Malabry, France

(Received 4 April 1984; accepted 19 June 1984)

The higher second-harmonic efficiency, in powder, of a new organic molecular crystal *N*-(4-nitrophenyl)-(*L*)-prolinol (NPP) is reported. Electronic polarizability of NPP molecules relates to that of other *para*-nitroaniline-like structures such as that of previously reported *N*-(2,4-dinitrophenyl) methyl alaninate (MAP), and the increase in crystalline nonlinear efficiency by one order of magnitude above the latter is ascribed to an "optimized" crystalline structure rather than to minor changes of the molecular hyperpolarizability. The simultaneous chiral and hydrogen-bonding character of the prolinol electron-donating group leads to a quasioptimal angle, with respect to quadratic phase-matched nonlinear interactions, between the molecular transition dipole moments and the twofold axis of the monoclinic $P2_1$ crystal structure. Based on a simple oriented gas description of the quasiplanar structure of the crystal, two possible mutually exclusive second-harmonic phase-matched configurations are evidenced and shown to promote the optimized nonlinear tensor coefficient.

I. INTRODUCTION

During the last decade, the search for new efficient nonlinear optical materials has led to the extensive investigation of relevant organic compounds.[1–7] The interest is driven by a number of potential applications[8,9] such as: second-harmonic generation, frequency-mixing, electrooptic modulation, optical parametric oscillation, etc.

Some organic materials exhibit efficiencies at least one order of magnitude above that of classical inorganic materials such as KDP or $LiNbO_3$. Other favorable features of organic materials for second-harmonic generation and related applications are their comparatively higher damage thresholds and the great variety of available chemical modifications among which some are capable of specifically enhancing a desired physical property. Characteristic of molecular crystal is also the fact that molecules, in their ground and even to some extent in their excited states, tend to remain well defined entities in the solid.[10,11]

In practice, the search for new organic materials proceeds in two related steps: molecular structure engineering and crystal structure engineering, the principles of which will be briefly recalled in Sec. II A and exemplified for paranitroaniline with the new concept of potentially hydrogen-bonding groups attached to the molecular structure. The prevailing contribution of hydrogen bonds to the definition of the molecular packing of the crystal will be considered as an extension of previously defined strategies (such as chirality) meant to prevent centrosymmetry and, furthermore, ideally ensure optimized dipolar orientations within the crystalline unit cell. This approach has eventually led us to a new material: NPP [for *N*-(4-nitrophenyl)-(*L*)-prolinol] (Sec. II B). The nonlinear response of this material will be seen to be one order of magnitude above that of currently developed molecular crystals for quadratic nonlinear optics such as MAP (for *N*-(2,4-dinitrophenyl) methyl alaninate). The crystalline structure of the material is detailed in Sec. III, evidencing a quasi-one-dimensional and highly stratified packing. This enhanced nonlinear response is subsequently analyzed in Sec. IV in terms of the very specific features of the crystalline structure. Predictions as to the birefringency and the geometry of the two only possible phase-matched configurations of the material are presented, based on an "oriented-gas" description.

II. MOLECULAR ENGINEERING OF NPP

A. Chiral hydrogen bonding nitroaniline derivatives for nonlinear optics

A number of models and related experiments have singled-out the relevance of internal charge transfer conjugated molecules (such as paranitroaniline derivatives) for efficient optical nonlinear effects within the 0.5, 2 μm transparency domain.[12–33] A two-level model of the electronic transitions of such molecules accounts well for their nonlinear properties[33(a)] at the microscopic level, laying the foundations of a "molecular engineering" approach to serve as a predictive guideline for further synthesis.

An additional necessary condition to prevent the second-order coefficient *d* from vanishing at the crystalline level, is the noncentrosymmetry of the crystalline structure met on the average by only 20% of molecular organic crystals.[34–36]

The impossibility to infer with absolute certainty from the sole inspection of the molecular structure the geometry of the crystalline packing[37,38] owing to the numerous and rather smooth atom–atom van der Waals interaction poten-

0021-9606/84/214160-08$02.10

tials accounting for it, can be successfully bypassed in some cases by a further structural engineering[31,32] approach of the problem. Success in this approach relies in some cases more on statistics than on purely deterministic theory-based predictions. An experimental screening powder test[39] to experimentally rule-out inefficient structures and further classify, selected ones, following a semiquantitative efficiency hierarchy, is still needed. The following strategies have already been attempted with reasonable success:

One of them is chirality: Molecular crystals built from a single enantiomer of a chiral compound necessarily exhibit a noncentrosymmetric structure although it does not ensure the alignment required for optimized nonlinear properties as defined in Ref. 33(b). MAP[4] is the first highly efficient nonlinear material exemplifying this principle.

Another strategy relies on the hypothesis that packing forces can be better controlled when molecules with vanishing dipole moments are involved.[3] In the absence of dipole–dipole interactions the packing is made more sensitive to the influence of minor molecular van der Waals modifications which may help rotate the molecules out of centrosymmetry. In a first step, we have studied achiral molecules exhibiting such a characteristic, and eventually found POM[3,40,41] (3-methyl-4-nitropyridine-1-oxyde) among a number of potentially interesting pyridine-oxyde derivatives.

Recently a third strategy has been successfully proposed by Meredith.[42] A number of molecular salts were investigated, with a stilbazolium cation shown to exhibit the proper electronic structure for enhancing the value, associated with a variety of anions. This method has resulted, after selection of the suitable anion (methylsulfate) in an optimized noncentrosymmetric structure.

Nitroaniline derivatives are among the most widely investigated organic materials in nonlinear optics.

Introduced first of all was metanitroaniline (mNA),[43–47] although the relative positions of the amino and nitro groups is not favorable to an efficient charge transfer. *Para*-nitroaniline (*p*-NA) has no potential for second-harmonic generation in view of its centrosymmetric crystalline structure but the corresponding molecular susceptibility was extensively studied, as *p*-NA may serve as a typical model of an intramolecular charge-transfer molecule.[20,24,26,31] 2,4-Dinitroaniline (DNA) is a very similar molecule for which the first order hyperpolarizability ($\beta = 21.10^{-30}$ esu)[29] is comparable to that of *para*-nitroaniline. MAP,[4] already mentioned for its remarkable nonlinear properties, is a derivative of DNA, made chiral in order to present centrosymmetry. An achiral derivative of *p*-NA, namely MNA (for 2-methyl-4-nitroaniline)[48,49] was reported for its unusually large coefficients. It is of interest to note that, in this compound, the sole methyl group in the 2-position suffices to circumvent *p*-NA's centrosymmetry and, moreover, ensures a very optimized crystalline structure. Permanent molecular dipole moments of *p*-NA derivatives are high ($\mu_g = 6.9$ D for *p*-NA) which might partially account for the small number of suitable crystallographic structures encountered when scanning achiral derivatives of *p*-NA: *N,N*-dimethylparanitroaniline, for example, crystallizes in the noncentrosymmetric space group $P2_1$ but leads to very low d coefficients owing to a quasi-antiparallel molecular packing in the unit cell.[64]

We report here the engineering of a new organic crystal builtup from *p*-NA derived molecules, and exhibiting an exceptionally large second-order response: in the present approach the molecular unit is given both chiral character and the potential to form, in the crystal phase, intermolecular hydrogen bonds. The main reason for systematically resorting to potentially hydrogen-bonding groups located within the nonlinear molecules is based on the following conjecture: as already mentioned, the high rate of centro or pseduocentrosymmetric structures encountered when scanning dipolar nonlinear molecules is, at least partially due to the influence of dipole–dipole interactions. If POM exemplifies a strategy which aimed at overcoming that tendency by cancellation of the dipole moment, NPP represents a symmetric approach to the same problem: dipole–dipole interactions are dominated more energertic interactions such as caused by hydrogen bonding. Of course in both approaches, the final interaction potentials meant to exert a prevailing influence on the molecular structure (i.e., van der Waals atom–atom potentials for POM and hydrogen bonding for NPP) are, as opposed to dipole–dipole electrostatic interactions, perfectly neutral as to the centro or noncentrosymmetric nature of the resulting crystalline structure. Actually, as will be published in a forthcoming paper, the rate of noncentrosymmetric structures for potentially hydrogen-bonding *p*-NA derivatives (such as amino-alcohol derivatives) raises significantly above 20% thus statistically supporting our new engineering approach.

B. The NPP molecule: Synthesis and properties

We have synthetized a series of chiral *p*NA derivatives using nucleophilic aromatic substitution, a well known organic reaction (ArSN reaction).[50]

The reaction is greatly favored by a strongly electron withdrawing substituent on the aromatic ring, so that nitroaromatics are the best substrates for nucleophilic aromatic substitution.

The reaction scheme is then:

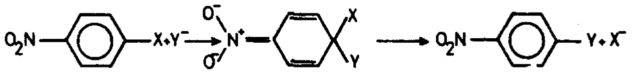

X is a potentially leaving group, and for example, fluoride behaves often as a more easily leaving group than other halogens, in the ArSN reaction.

That is why 1-fluoro-4-nitrobenzene was used as the starting material, according to previously described procedures.[50,51] The use of chiral natural aminoacids as nucleophile compounds often led to noncrystalline compounds, and the resulting series were forsaken. Then chiral aminoalcohols derived from natural aminoacides were used as well as other easily available chiral aminoalcohols such as (−) ephedrine etc., in order to keep a hydroxy group for the expected hydrogen bonding.

Among the numerous chiral *p*NA derivatives we have prepared accordingly, (*S*)(−)-2-hydroxymethyl-1-(4-nitrophenyl)-pyrrolidine [which we shall call NPP further on, for *N*-(4-nitrophenyl)-(*L*)-prolinol], stands out as the most efficient second-harmonic generator in this class of material at the powder stage. The synthesis is detailed in Appendix A, following the scheme below:

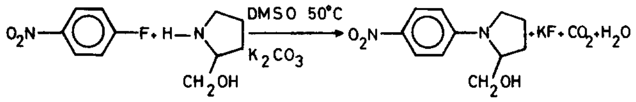

Like all *N,N*-disubstituted *p*NA derivatives, NPP displays an intense charge-transfer absorption band in the near ultraviolet: $\lambda_{\max} = 390$ nm in ethanol ($\epsilon_{\max} = 18\,700$) (see Fig. 1).

This electronic absorption band has been extensively studied: its location is very solvent dependent, from 323 nm in nonpolar solvents, up to 385 nm in polar solvents for *p*NA.[52–56] The absorption of thin single crystals of *p*NA has been also undertaken, first by Tanaka,[57] and more recently by Bertinelli *et al.*[58] demonstrating the complexity of the excitonic structure of *p*NA single crystal spectrum. The authors observed an intense absorption at 370 nm in the crystal spectrum, closer to what is observed in polar rather than in nonpolar solvents.

The absorption behavior of a 10^{-2} M solution of NPP in methanol filling a 1 cm thick cell should accordingly show qualitative features similar to that of a 16 μm thick crystalline sample, an estimation based on molecular packing data detailed in Sec. III. In comparison, the absorption edges of two other reference organic compounds previously studied (MAP and POM) are given in Fig. 2. The NPP cut-off wavelength is red shifted, as compared to that of POM and MAP by about 20 nm. The 90% transmittance observed at 0.53 μm qualifies this new material as an efficient doubler of the 1.06 μm YAG : Nd^{3+} laser emission. NPP crystal growth attempts are presently under way. NPP melts at 116 °C and is readily soluble in a number of simple solvents. Encouraging results in this direction will be published in a forthcoming paper, together with crystalline nonlinear coefficients.

III. CRYSTAL AND MOLECULAR STRUCTURE OF NPP

A. Crystal data

The crystal structure of NPP ($C_{11}H_{14}N_2O_3$) is monoclinic with space group $P2_1$ and parameters: $a = 5.261(1)$, $b = 14.908(3)$, $c = 7.185(2)$ Å, $= 105.18(2)°$. The volume of the unit cell is $V = 543.8(\text{Å})^3$. The molecular weight of NPP is $M = 222$ and the crystal, with two molecules in the unit cell, has a calculated density $D = 1.36$ g cm^{-3}.

The intensity data were obtained with a single crystal having the shape of a truncated pyramide (0.5 mm high and $0.2 \times 0.2 \times 0.3$ mm at the middle section). The radiation used is Cu-*Kα*, ($\lambda = 1.542$ Å) and the linear absorption coefficient is $\mu = 7.4$ cm^{-1}. The intensities of 1095 independent reflexions were measured on a CAD-4 ENRAF NONIUS automatic diffractometer. The scanning of the reciprocal space lies in the range: $-6 < h < 0$, $-8 < l < 8$, and $-18 < k < 0$ ($\sin\theta/\lambda < 0.37$). Among these reflections, 31 were considered as unobserved [$I < 2\sigma(I)$].

The structure was resolved by a direct method using the program MULTAN 80.[59] The refinement was performed with a least-square procedure using the program SHELX 76.[60] The hydrogen atoms were introduced *a priori* with calculated positions (the distances C–H are fixed to 1.08 Å and the distance O(3)–H(14) to 0.97 Å). In the final stages, the non hydrogen atoms were refined with anisotropic thermal parameters and hydrogen atoms were assigned the fixed isotropic thermal parameters of the attached carbon atoms. The thermal parameters lie in the correct range (0.04, 0.07 Å) except those for the atoms O(2) ($U_{11} = 0.10$ Å^2, $U_{22} = 0.08$ Å^2). Six reflections were eliminated because $|F(\text{obs})-F(\text{calc})|\rangle 4\sigma$[(00-2), (23-5), (01-2), (53-4), (44-3), (−11-1)]. The final R index is 0.050 for 1058 reflexions. The atomic positions together with their standard deviations are given on Table I.

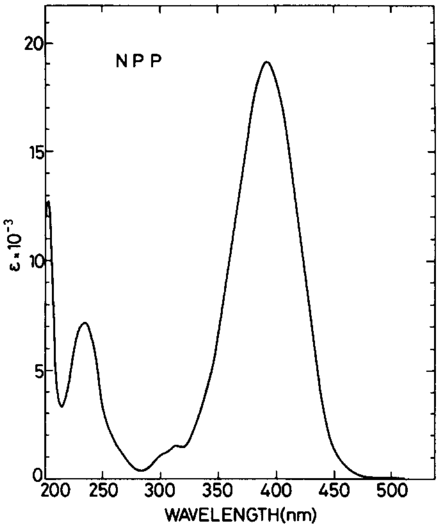

FIG. 1. Electronic absorption spectrum of NPP in ethanol at 20 °C.

B. Molecular configuration (Figs. 3–5)

The molecule of NPP is derived from that of paranitroaniline and it is interesting to compare the former with both the structures of 4-nitroaniline (Trueblood *et al.*,[62] revisited by Colapietro *et al.*[63]) and *N*, *N*-dimethyl-*p*-nitroaniline.[64]

The benzene ring is planar with an excellent precision: (the maximum departure from the C-atom plane is 0.008 Å and the standard deviation is 0.005 Å. Both nitrogen atoms N(1) and N(2) are slightly out of the aromatic plane on the same side (by 0.01 and 0.04 Å, respectively). The nitro group

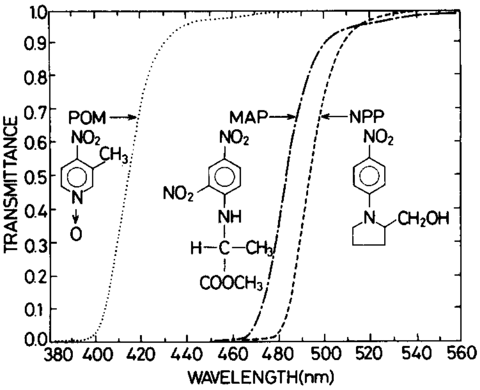

FIG. 2. Absorption cutoffs of 10^{-2} M solutions in methanol of NPP, MAP, and POM.

TABLE I. Atomic coordinates (fractional values) with standard deviations magnified by a 10^5 factor for all atoms except hydrogen 14 (10^4).

Atom	$x(\sigma x)$	$y(\sigma y)$	$z(\sigma z)$
C1	0.5228 (4)	0.0095 (2)	0.4364 (3)
C2	0.5340 (4)	− 0.0840 (2)	0.4508 (3)
C3	0.6587 (4)	0.1319 (2)	0.3385 (3)
C4	0.7763 (4)	0.0887 (2)	0.2067 (3)
C5	0.7657 (5)	− 0.0063 (2)	0.1971 (4)
C6	0.6395 (5)	− 0.0543 (2)	0.3104 (3)
C7	0.8705 (4)	0.2340 (2)	0.0635 (3)
C8	0.9035 (5)	0.2455 (2)	− 0.1410 (3)
C9	1.0918 (5)	0.1708 (2)	− 0.1592 (3)
C10	1.0062 (4)	0.0925 (2)	− 0.0531 (3)
C11	1.0788 (4)	0.2850 (2)	0.2129 (3)
N1	0.3908 (4)	− 0.0588 (2)	0.5543 (3)
N2	0.8957 (4)	0.1360	0.0914 (3)
O1	0.3614 (4)	− 0.1407 (2)	0.5325 (3)
O2	0.3080 (5)	− 0.0179 (2)	0.6767 (3)
O3	1.0587 (4)	0.3786 (2)	0.1809 (3)
H14	0.921 (5)	− 0.403 (3)	0.233 (5)

is coplanar with the attached carbon and it is twisted about the C–N bond by 5.8° [the atoms O(2) and O(3) lie in the same side of the aromatic plane].

The amino-group is clearly not planar: the nitrogen N(2) is 0.10 Å out of the C(4)C(7)C(10)-plane which indicates a slightly but significant pyramidal hybridization of the amino nitrogen. That is an original feature in comparison with 4-nitroaniline[61] and *N*, *N*-dimethyl-4-nitroaniline[64] where the amino group is found planar.

The bond lengths of the benzene ring are in good agreement with those given in the referenced structures.[63–65] The distance C(4)–N(2) in NPP(1.361 Å) confirms the remarkable rigidity of the C–N (amino) bond in these compounds where the corresponding length are in the range: 1.352–1.358 Å. On the other hand the C–N (nitro) bond seems more influenced by the substituent: the corresponding bond length is 1.400 Å in *N*,*N* dimethyl-4-nitroaniline[64] and 1.466 Å in 2,6 dichloro-4-nitroaniline[65]; in NPP the distance C(1)–N(1) is 1.439 Å which is almost identical to the value given by Colapietro *et al.* for paranitroaniline[63] (it is slightly different from that given by Trueblood *et al.*[62] for the same structure: 1.454 Å). These results evidence a strong relationship between NPP and paranitroaniline and the distances are consistent with a predominant contribution of a quinonoid form.

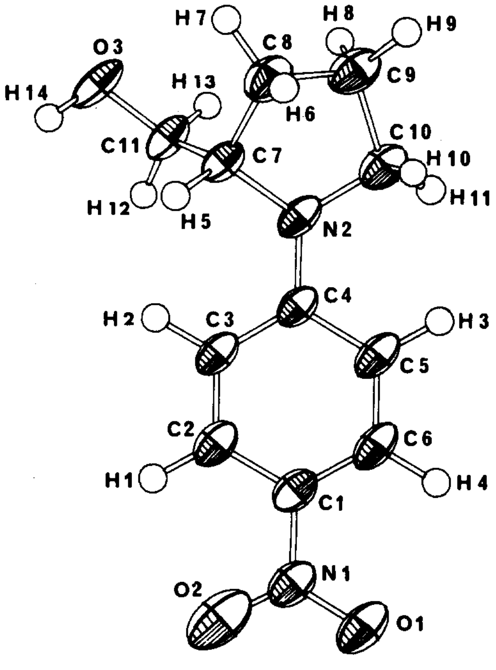

FIG. 3. Molecule of NPP projected on the aromatic plane. Plotted with the program ORTEP (Johnson, 1965). the thermal ellipsoids being at the 50% probability level (hydrogen atoms excepted).

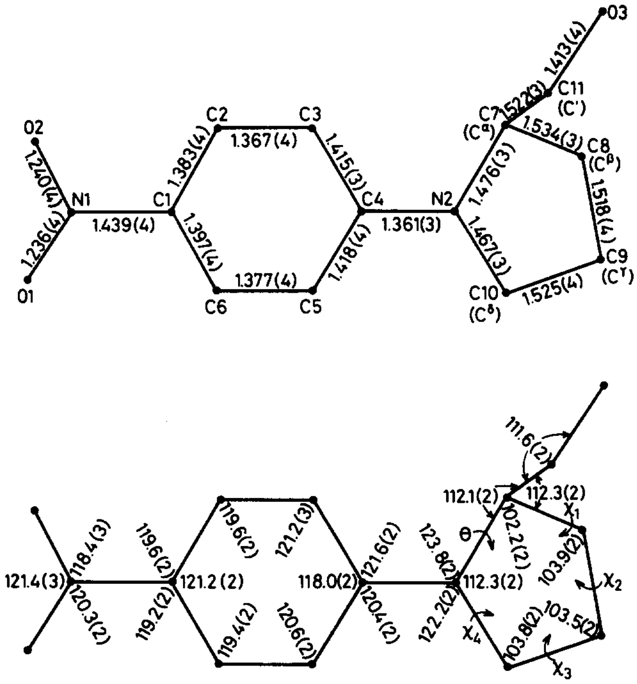

FIG. 4. Bond lengths and angles (hydrogen atoms omitted). The IUPAC-IUB (Ref. 61) convention is used for designation of atoms (in parentheses) and torsion angles of the pyrrolidine ring. Torsion angles for the pyrrolidine ring $\theta = -14.7°$, $X_3 = 28.6°$, $X_1 = 32.2$, $X_4 = -8.5°$, $X_2 = -38.1°$.

There are several possible configurations for the pyrrolidine ring. In NPP, the ring has a C2–C-endo configuration according to the nomenclature introduced by Ashida and Kakudo.[66] The ring thus exhibits an approximate C2 symmetry (half-chair) with a twofold axis passing through N(2) and the midpoint of the C(7)–C(8) bond. The carbon C9 is out of the C(10)N(2)C(7) plane on the same side as the carbon C(11) (see Fig. 5). It is a conformation *B* according to the classification of Balasubramanian *et al.*[67] The bond length, angles, and torsion angles (see Fig. 4) are in good agreement with the values given in the literature except the above-mentioned weakly pyramidal nitrogen bond which is a very unusual arrangement in the pyrrolidine ring.

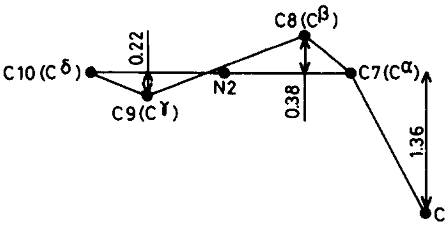

FIG. 5. Pyrrolidine ring as viewed from atom N_2.

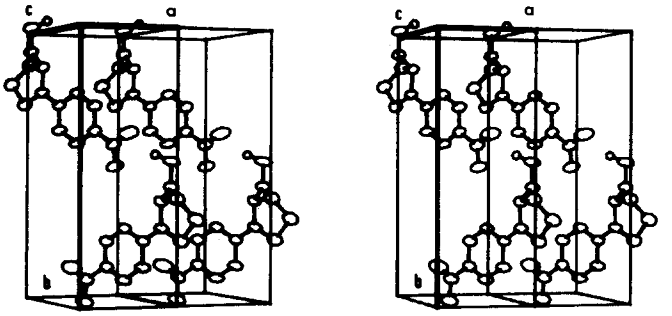

FIG. 6. Stereodrawing of the molecular packing in the NPP crystal.

C. Packing (Figs. 6 and 7)

The most interesting feature of the packing is the proximity of the mean plane of the molecule with the crystallographic plane (101), the angle between both of these planes being 11°. This particular arrangement, shown in Fig. 7, suggests that the (101) plane is a possible cleavage plane. Inside this plane the structure is characterized by infinite hydrogen bond chains along the binary axis. This hydrogen bond O(3)–H(14)···O(2) connects the hydroxyl group with the nitro group of the upper-adjacent molecule and the distance O(3)–O(2) (2.86 Å) corresponds to a bonding of medium intensity. Other shorter interatomic distances are within the expected values for van der Waals contacts. The angle between the charge transfert axis N(1)–N(2) and the binary axis is 58.6°, which will be shown in Sec. IV to be highly favorable to nonlinear interactions in the compound.

IV. ORIGIN OF THE HIGH NONLINEAR RESPONSE OF NPP POWDER MATERIAL

NPP powder samples were tested in second-harmonic generation following the semiquantitative procedure described by Kurtz *et al.*[39] The source used here is a mode-locked picosecond YAG laser. The 1.06 μm pulse selected from the train has duration 30 ps and average energy 1 mJ. The unfocused fundamental beam shining the sample has 2.5 mm radius. The powder is located in between two transparent glass plates and sample thicknesses (2 mm) are kept constant in all subsequent experiments. The sample is located at the focus of a parabolic silver plated reflector which reflects back into the photomultiplier the backscattered harmonic wave. The fundamental is filtered out after interaction. The energy fluctuation between pulses demands the use of a reference sample shined by a portion of the fundamental pulse. The reference used here is a calibrated powder of quartz (grain size ranging from 50 to 100 μm). The harmonic power signal from the sample is divided by that from the reference to yield a fluctuation-free value of the nonlinear efficiency ratio. Table II yields nonlinear efficiency ratios for a number of organic powders including NPP. Ortho-NPP (see Appendix A), urea(68), MAP(4), and NPP display nonlinear efficiencies, respectively, of the same order of magnitude, one, two, and three order of magnitude above that of the quartz reference sample. In all cases, the results of Table II show an increased, or stable value (for MAP) of the nonlinear efficiency ratio when increasing the average grain dimension. This is consistent with analysis of Ref. 39 for phase-matchable materials, as summarized in Fig. 7 of that same reference. The statistical model of phase-matched interactions in powders developed in Part C of Ref. 39 is consistent with one single dominant phase-matching orientation present at a given wavelength of experimental interest. A more detailed analysis of the structure of NPP, making use of additional dielectric considerations, predicts, as will be shown in the following two mutually exclusive such priviledged phase-matching directions. Furthermore, these directions will be shown to take advantage of an optimized crystalline nonlinear coefficient. The very high response of the material as compared to that of MAP, of a similar molecular nature, but less favorable in terms of crystal packing, can thus be accounted for. Considering the anisotropy of the NPP molecule induced by the highly directional (donor prolinol group-acceptor nitro group) interaction, we shall assume in the following (according to notations on Fig. 8):

$$\alpha_{aa} > \alpha_{bb} > \alpha_{cc}, \qquad (2)$$

where α_{ij} stands for the molecular polarizability and (a,b,c) is a "natural" molecular reference frame. For a matter of further simplification we shall assume that the X,Y,Z frame coincides with the dielectric frame XYZ, which amounts to neglecting the probably minor contribution of the out-of-plane bonds (namely the methanol termination of the prolinol substituent group) to the dielectric tensor.

This assumption relies on the crystallographic data of Sec. III, showing a quasiplanar-NPP molecule in coincidence with the mean molecular plane ZX(101).

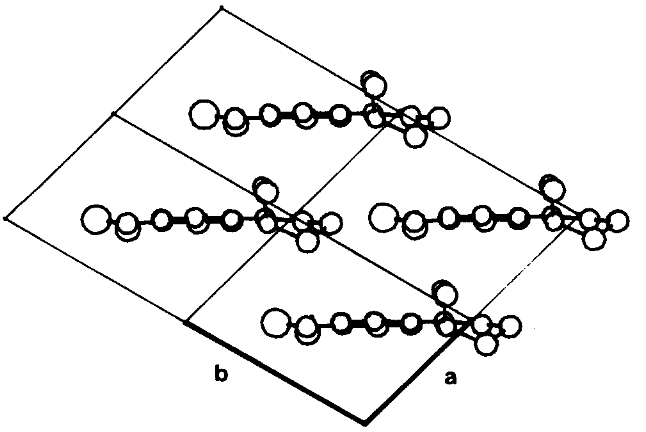

FIG. 7. Projection along axis 2_1 (b), showing a planar packing of the molecules in the structure (the representation is restricted to only one molecule per unit cell).

TABLE II. SGH powder test results for a number of organic compounds, scaled to the response of a calibrated quartz powder.

Compound	Grain Caliber (μm)	Efficiency
Ortho-NPP	···	1–1,5
Urea	120–150	20
Urea	150–200	40
Urea	200–350	70
MAP	200–350	200
MAP	350–500	200
NPP	150–200	2000
NPP	200–350	3500

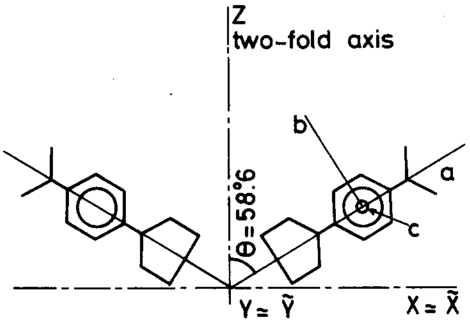

FIG. 8. Point-group simplified representation of the NPP monoclinic unit cell with a along the mean intramolecular charge transfer axis (connecting N_1 to N_2) and b perpendicular to a within the mean molecular plane. Z is the crystal twofold axis.

Introducing the crystalline polarizability per molecule a_{IJ} and following an oriented gas model approach as defined in Ref. 33(a), leads to

$$a_{XX} = \sin^2\theta\alpha_{aa} + \cos^2\theta\alpha_{bb}, \tag{3}$$

$$a_{ZZ} = \cos^2\theta\alpha_{aa} + \sin^2\theta\alpha_{bb}, \tag{4}$$

$$a_{YY} = \alpha_{cc}. \tag{5}$$

Subtracting expressions (3) and (4) yields a positive value for $a_{xx} - a_{zz}$:

$$a_{XX} - a_{ZZ} = \cos 2\theta\,(\alpha_{bb} - \alpha_{aa}) > 0 \tag{6}$$

both $\cos 2\theta$ and $\alpha_{bb} - \alpha_{aa}$ being negative. Besides

$$a_{ZZ} = \cos^2\theta\alpha_{aa} + \sin^2\theta\alpha_{bb} > (\cos^2\theta + \sin^2\theta)\alpha_{bb} > \alpha_{cc} = a_{yy}. \tag{7}$$

In summary:

$$a_{XX} > a_{ZZ} > a_{YY}. \tag{8}$$

Determination of the birefringency associated with these polarizabilities follows from application of the Clausius–Mosotti or Lorenz–Lorentz relation[69]:

$$a_{\rm II} = \frac{3}{4\pi N}\frac{n_{\rm I}^2 - 1}{n_{\rm I}^2 + 2}, \quad I = X,Y,Z \tag{9}$$

or

$$n_{\rm I} = \left[\frac{3 + 8\pi{\rm N}a_{\rm II}}{3 - 4\pi{\rm N}a_{\rm II}}\right]^{1/2}, \quad I = X,Y,Z, \tag{10}$$

where N is the number of molecules per unit volume of the crystal. Noticing that $n_{\rm I}$ is increasing with $a_{\rm II}$ (for physically relevant positive values of $a_{\rm II}$), the following set of index inequalities is ensured:

$$n_X^\omega > n_Z^\omega > n_Y^\omega. \tag{11}$$

This index ordering will be assumed to hold for all ω. Let us now analyze, in view of these previous dielectric inequalities, the origin and symmetry of the highly efficient phase-matched response of the powder material. Two situations are encountered, with different consequences in terms of the phase-matching potential of the material.

Distinction between the two situations is based on the comparison between the dispersion of refractive index n_Z and in-plane birefringency $n_X^\omega - n_Z^\omega$. First (respectively second) possibility, with the corresponding detailed view of the double-sheeted index surface on Fig. 9.I (respectively 9.II) assumes:

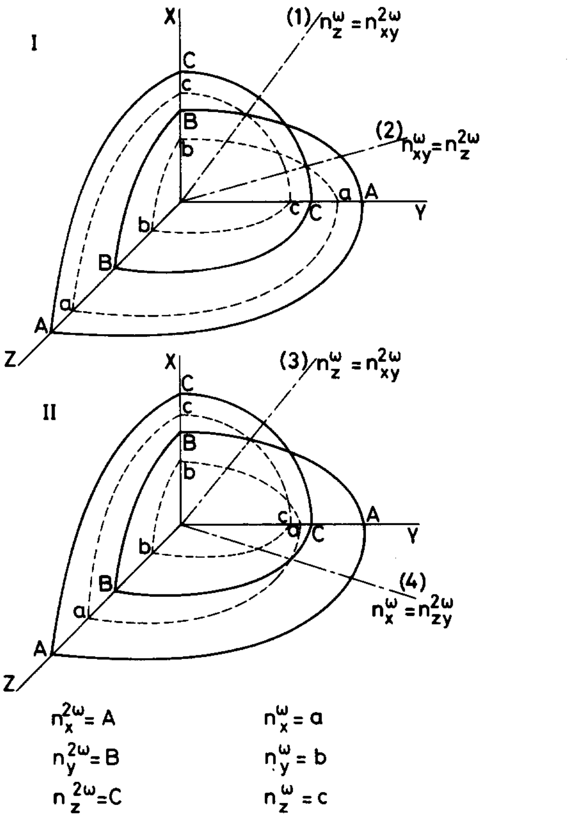

FIG. 9. Representation of the index surface of NPP in two cases: 9.I: $n_Z^{2\omega} - n_Z^\omega < n_Z^\omega - n_Z^\omega$, 9.II: $n_Z^{2\omega} - n_Z^\omega > n_Z^\omega - n_Z^\omega$. The four apparent phase-matching configurations are displayed, out of which two only (namely, 2 and 4) appear compatible with symmetry requirements.

$$n_Z^{2\omega} - n_Z^\omega < n_X^\omega - n_Z^\omega \tag{12}$$

$$(\text{respectively } n_Z^{2\omega} - n_Z^\omega > n_X^\omega - n_Z^\omega), \tag{13}$$

and points-out two apparently possible phase-matching directions namely Eqs. (1) and (2) [respectively (3) and (4)]. Possibility (1) is forbidden for simple symmetry reasons: it requires matching the index of an "ordinary" Z-polarized fundamental field with that of an "extraordinary" (X,Y)-polarized harmonic field to ensure: $n_Z^\omega = n_{XY}^{2\omega}$. The requirement cannot be fulfilled by the following set of nonlinear equations, complying with the $P2_1$ and Kleimman(70) symmetry constraints:

$$P_X^{2\omega} = 2d_{14}E_Y^\omega E_Z^\omega + 2d_{31}E_X^\omega E_Z^\omega, \tag{14}$$

$$P_Y^{2\omega} = 2d_{32}E_Y^\omega E_Z^\omega + 2d_{14}E_X^\omega E_Z^\omega, \tag{15}$$

$$P_Z^{2\omega} = d_{31}(E_X^\omega)^2 + d_{32}(E_Y^\omega)^2 + 2d_{14}E_X^\omega E_Y^\omega, \tag{16}$$

As can be seen from inspection of Eqs. (14) and (15), a purely z-polarized E_ω field cannot generate $a(X,Y)$ harmonic polarization $P^{2\omega}$. Possibility (2) is associated with the synchronization of a $(X-Y)$ polarized fundamental field with a Z-polarized harmonic field requiring $n_Z^{2\omega} = n_{XY}^\omega$. Calling θ_2 the angle between the Y axis and the phase-matching propagation direction, this situation corresponds to an effective d coefficient:

$$d_{\text{eff}} = d_{31}\cos^2\theta_2 + d_{32}\sin^2\theta_2 + 2d_{14}\sin\theta_2\cos\theta_2. \tag{17}$$

Using a simplified one-dimensional description of the molecular nonlinear tensor of the NPP molecule,[33(b)] it is possible to further order the magnitude of the crystalline nonlinear coefficients: let us assume for simplification that the third-rank tensor β has only one non vanishing coefficient along the charge transfer axis a (see Fig. 8), namely β_{aaa}. Using again an oriented gas description of the solid leads to

$$d_{31} = N\beta_{aaa}\cos\theta\sin^2\theta, \tag{18}$$

$$d_{33} = N\beta_{aaa}\cos^3\theta \tag{19}$$

all other coefficients being negligible (θ is defined according to Fig. 8).

Furthermore the angular projection factor weighing β_{aaa} in Exp(18) is maximized for $\theta \simeq 54.74°$, a value which comes close to the actual θ value: 58.6° (see Sec. III). In that sense, d_{31} may be considered as an "optimized" nonlinear coefficient. Any phase-matching configuration emphasizing this coefficient is thus to be considered as highly desirable. Note that similar optimization of d_{33}, corresponding to $\theta = 0$ (weighing factor to be optimized: $\cos^3\theta$) would be of no use for birefringence phase matching.

In the present situation [case (2)] one ends up, under the previous approximations with a simplified expression for d_{eff} namely: $d_{\text{eff}} \simeq d_{31}\cos^2\theta_2$.

A "mixed" optimization, achieving a trade off between d_{33} and d_{31} has been also obtained in the aforementioned stilbazolium salt,[42] and corresponds to a θ value of 34°.

This configuration is thus seen to promote, as desired, the optimized d_{31} coefficient.

This situation would be made even more attractive by a weak θ_2 value: the phase-matching configuration would then be near to noncritical and d_{eff} come close to the optimized d_{31}, coefficient.

Such an ideal situation would correspond to the exact compensation of the (XZ) plane birefringency by the Z dispersion, i.e.,

$$n_Z^{2\omega} - n_Z^{\omega} = n_X^{\omega} - n_Z^{\omega}.$$

Situation (3) is to be discarded for considerations strictly identical to those encountered for (1). In case (4) a X-polarized fundamental field is to be synchronized with a $(Y\text{–}Z)$-polarized harmonic field, $(n_X^{\omega} = n_{YZ}^{2\omega})$, which is compatible with Eqs. (14)–(16). Calling θ_4 the angle between Y and the phase-matched propagation direction, the effective nonlinear coefficient is

$$d_{\text{eff}} = \cos\theta_4 d_{31}. \tag{20}$$

The same considerations as for case (4) apply here including the potential interest of a hopefully small value for θ_4 and the prevailing contribution of the optimized d_{31} coefficient to the phase-matched energy transfer.

Summing up the analysis of the four possible situations encountered, only cases (2) and (4) are symmetry allowed and both promote the optimized d_{31} coefficient. Cases (2) and (4) exclude each other as corresponding to $n_Z^{2\omega} - n_Z^{\omega}$, respectively, inferior and superior to $n_X^{\omega} - n_Z^{\omega}$.

IV. CONCLUSION

The notion of an optimized crystalline structure for phase-matched bulk quadratic nonlinear interactions has been exemplified here by a new molecular crystal: N-(4-nitrophenyl)-(L)-prolinol (NPP). The molecular electronic properties of NPP relate to that of paranitroaniline analogs and the higher SHG nonlinear efficiency observed in powder (one order of magnitude above that of MAP) cannot be ascribed to significant variations of the molecular susceptibility. The conjunction of chirality and hydrogen bonding groups, as brought about by the electron donating aminoalcohol substituent group induces a much more symmetric type of crystalline packing than can be expected from a general monoclinic structure: molecules are attached to each other by hydrogen bonds in quasiplanar chains stacked in parallel crystalline planes parallel to the twofold symmetry axis. The angle between the symmetry axis and the transition dipole moments (58°6) comes close to the optimal angle (54.74°) for quadratic phase-matched interactions with orthogonal ω and 2ω polarizations parallel to the molecular plane.

This configuration results in an optimal d_{ZXX} coefficient, assuming a fairly constant average value of the molecular susceptibility for paranitroaniline analogs.

Based only on SGH powder test results, we show that careful dielectric analysis of the dielectric properties of the crystal, made simpler by its highly stratified anisotropic packing, helps identify possible phase-matched configurations at a given wavelength. Both of the possible mutually exclusive configurations promote the optimized d_{ZXX} coefficient. Crystal growth studies are presently undertaken: we expect, following preliminary experiments, the already promising potential of this material to be further increased by non critical phase-matching along Y (i.e., propagation perpendicular to the mean molecular plane) in the near I.R. range.

ACKNOWLEDGMENTS

It is a pleasure to acknowledge the support of H. Le Person for the powder-test measurement and numerous discussions with J. Badan, R. Hierle, I. Ledoux, A. Perigaud, and P. Vidakovic.

APPENDIX A

The preparation procedure of NPP is detailed here: we placed L-prolinol (25 g, 0.247 mol, JANSSEN CHIMICA), 25 ml of freshly distilled dimethylsulfoxyde (DMSO), and one equivalent of potassium carbonate (K_2CO_3) in a 250 ml round bottom two-necks-flask, equipped with a stirring bar. A solution of 1-fluoro-4-nitrobenzene (FNB : 33 g, 0.235 mol, JANSSEN CHIMICA) in 25 ml of DMSO was slowly added with stirring. The resulting mixture has been heated for 24 h at 50 °C, with stirring. CO_2 evolution is observed. After this time, only a trace of FNB is detected by thin layer chromatography (silica plates, eluent ether). After cooling, the reaction mixture is poured in 800 ml of cold water, with vigorously stirring. The yellow solid is collected by filtration and dried under vacuum: 48 g is obtained (yield 92%).

This crude material is recrystallized with chloroforme–cyclohexane (2-1) or toluene, after treatment by activated charcoal. A light yellow solid in the shape of thin whiskers is collected and dried under vacuum (46 g; overall yield 87%). A number of physico-chemical data were measured:

mp : 116°C; $[\alpha]_D^{20} - 92.1°([\phi]_D^{20} - 204.7°)(c = 1$, absolute EtOH).
Ir (nujol mull) : 3440-1590-1300-1280-1100-1050 cm^{-1}.
1H NMR ($CDCl_3$, δ from TMS) : 2.10 (broad *s*, 5H); 3.25–3.70 (m,4H) 4.0 (broad *s*, 1H), 6.07 ($d,J = 9$ Hz,2H); 8.02 ($d,J = 9$ Hz,2H)
Analysis: Calcd for $C_{11}H_{14}N_2O_3$: C, 59.45; H, 6.35; N, 12.60.
Found: C,59.31; H, 6.41; N, 12.66. Mw = 222.24.

Great care should be given to the chemical purity of FNB. The presence of the ortho isomere, 1-fluoro-2-nitrobenzene, led to the ortho substituted compound, which was found to be an intense red crystalline compound (mp = 80/81 °C).

This colored product, easily detected by TLC analysis, should be carefully removed from NPP material, to avoid undesirable absorption.

[1] *Nonlinear Optical Properties of Organic and Polymeric Materials*, edited by D. J. Williams, (ACS Symp. Ser. 233, Washington D. C. 1983).

[2] J. Zyss, J. Non-Cryst. Solids **47**, 211 (1982).

[3] J. Zyss, D. S. Chemla, and J. F. Nicoud, J. Chem. Phys. **74**, 4800 (1981).

[4] J. L. Oudar and R. Hierle, J. Appl. Phys. **48**, 2699 (1977).

[5] K. Jain, J. I. Crowley, G. H. Hewig, Y. Y. Cheng, and R. J. Tweig, Opt. Laser Technol. **13**, 297 (1981).

[6] R. Tweig, A. Azema, K. Jain, and Y. Y. Cheng, Chem. Phys. Lett. **82**, 208 (1982).

[7] A. F. Garito and K. D. Singer, Laser Focus **59** (1982).

[8] N. Bloembergen, *Non Linear Optics* (Benjamin, New York, 1965).

[9] H. Rabin and C. L. Tang, *Quantum Electronics* (Academic, New York, 1965).

[10] A. I. Kitaigorodskii, *Organic Chemical Crystallography* (Consultant Bureau, New York, 1961).

[11] J. N. Murrel, in *Orbital Theories of Molecules and Solids* (edited by N. H. March (Clarendon, Oxford 1974); The occurence of noticeable collective effects such as excitonic splitting, brought about by the periodic structure of the crystal can be neglected in on optical studies undertaken within the transparency range of the medium. Such is the case here where an "oriented gas" model may be applied satisfactorily.

[12] A. Schweig, Chem. Phys. Lett. **1**, 163, 195 (1967).

[13] F. N. H. Robinson, Bell. Syst. Technol. J. **46**, 913 (1967).

[14] D. L. Davydov, V. V. Dunina, V. F. Zolin, and G. Koreneva, Opt. Spectrosc. **34**, 150 (1973).

[15] J. L. Oudar and H. Le Person, Opt. Commun. **15**, 258 (1975).

[16] D. S. Chemla, J. L. Oudar, and J. Jerphagnon, Phys. Rev. B **12**, 4534 (1975).

[17] J. L. Oudar and D. S. Chemla, Opt. Commun. **13**, 164 (1975).

[18] J. L. Oudar, D. S. Chemla, and E. Batifol, J. Chem. Phys. **67**, 1626 (1977).

[19] J. L. Oudar, J. Chem. Phys. **67**, 446 (1977).

[20] J. L. Oudar and D. S. Chemla, J. Chem. Phys. **66**, 2664 (1977).

[21] B. F. Levine and C. G. Bethea, Appl. Phys. Lett. **24**, 445 (1974).

[22] B. F. Levine, J. Chem. Phys. **63**, 115 (1975).

[23] B. F. Levine and C. G. Bethea, J. Chem. Phys. **63**, 2666 (1975).

[24] B. F. Levine, Chem. Phys. Lett. **37**, 516 (1976).

[25] B. F. Levine and C. G. Bethea, J. Chem. Phys. **67**, 516 (1976).

[26] A. Dulcic and C. Sauteret, J. Chem. Phys. **69**, 3453 (1978).

[27] S. J. Lalama and A. F. Garito, Phys. Rev. A **20**, 1179 (1979).

[28] J. A. Morrell and A. C. Albrecth, Chem. Phys. Lett. **64**, 46 (1979).

[29] K. D. Singer and A. F. Garito, J. Chem. Phys. **75**, 3572 (1981).

[30] J. Zyss, J. Chem. Phys. **70**, 3333, 3341 (1979); **71**, 909 (1979).

[31] G. R. Meredith and B. Buchalter, J. Chem. Phys. **78**, 1938 (1983).

[32] D. S. Chemla, J. L. Oudar, and J. Zyss, Echo des Recherches, CNET, English issue, **47** (1981).

[33] (a) J. L. Oudar and J. Zyss, Phys. Rev. A **26**, 2016 (1982); (b) J. Zyss and J. L. Oudar, Phys. Rev. A **26**, 2028 (1982).

[34] D. Y. Curtin and I. C. Paul, Chem. Rev. **81**, 525 (1982).

[35] A. Gavezzotti and M. Simonetta, Chem. Rev. **82**, 1 (1982).

[36] I. S. Rez, Sov. Phys. Crystallogr. **5**, 63 (1960).

[37] P. Dauber and A. Hagler, Acc. Chem. Res. **13**, 105 (1980).

[38] T. V. Timofeeva, N. Y. Chernikova, and P. M. Zorkii, Russ. Chem. Rev. **49**, 509 (1980).

[39] S. K. Kurtz and T. T. Perry, J. Appl. Phys. **39**, 3798 (1968).

[40] M. Sigelle and R. Hierle, J. Appl. Phys. **52**, 4199 (1981).

[41] M. Sigelle, J. Zyss, and R. Hierle, J. Non-Cryst. Solids **47**, 287 (1982).

[42] G. Meredith, Polym. Prepr. Am. Chem. Soc. Div. Polym. Chem. **23**, 158 (1982) see also Design and Characterization of Molecular and Polymeric Nonlinear Optical Materials: Successes and Pitfalls in Ref. 1.

[43] J. L. Stevenson and A. C. Skapski, J. Phys. C **5**, L223 (1972).

[44] J. L. Stevenson, J. Phys. D **6**, L13 (1972).

[45] A. C. Skapski and J. L. Stevenson, J. Chem. Soc. Perkin Trans. 2 **1973**, 1197.

[46] P. D. Southgate and D. S. Hall, Appl. Phys. Lett. **18**, 456 (1971).

[47] K. Kato, IEEE J. Quantum Electron. **QE-16**, 1288 (1980).

[48] B. F. Levine, C. G. Bethea, C. D. Thurmond, R. T. Lynch, and J. L. Bernstein, J. Appl. Phys. **50**, 2523 (1979).

[49] G. F. Lipscomb, A. F. Garito, and R. S. Narang, J. Chem. Phys. **75** 1509 (1981).

[50] R. E. Parker, Adv. Fluorine Chem. **3**, 63 (1963).

[51] H. E. Smith, W. I. Cozart, T. de Paulis, and F. M. Chen, J. Am. Chem. Soc. **101**, 5186 (1979).

[52] R. R. Minesinger and M. J. Kamlet, J. Phys. Chem. **78**, 494 (1974).

[53] S. Millefiori, G. Favini, A. Millefiori, and D. Grasso, Spectrochim. Acta Part A **33**, 21 (1975).

[54] T. P. Carsey, G. L. Findley, and S. P. McGlynn, J. Am. Chem. Soc. **101**, 4502 (1979).

[55] O. S. Khalil and S. P. McGlynn, J. Lumin. **11**, 185 (1975–76).

[56] H. J. Freund and R. W. Bigelow, Chem. Phys. **55**, 407 (1981).

[57] J. Tanaka, Bull. Chem. Soc. Jpn. **36**, 833 (1963).

[58] F. Bertinelli, P. Palmieri, A. Brillante, and C. Talliani Chem. Phys. **25**, 333 (1977).

[59] P. Main, S. J. Fisfe, S. E. Hull, L. Lessinger, G. Germain, J. P. Declercq, and M. M. Woolfson (1980). MULTAN 80. A system of computer programs for the automatic solution of crystal structures from x-ray diffraction data. (Departement of Physics, University of York, England, and Louvain, Belgium.)

[60] G. M. Sheldrick (1976). SHELX. Program for crystal structure determination. (University of Cambridge, England.)

[61] IUPAC-IUB Commission on Biochemical Nomenclature, J. Mol. Biol. **52**, 1 (1970).

[62] K. N. Trueblood, E. Goldish, and J. Donohue, Acta Crystallogr. **14**, 1009 (1961).

[63] M. Colapietro, A. Domenicano, C. Marciante, and G. Portalone, Acta Crystallogr. Sect A **37**, C199 (1981).

[64] T. C. W. Mak and J. Trotter, Acta Crystallogr. **18**, 68 (1965).

[65] D. L. Hugues and J. Trotter, J. Chem. Soc. A **1971**, 2181.

[66] T. Ashida and M. Kakudo, Bull. Chem. Soc. Jpn. **46**, 1129 (1974).

[67] R. Balasubramanian, A. V. Lakshminarayanan, M. N. Sabesan, G. Tegoni, K. Venkatesan, and G. N. Ramachandran, Int. J. Protein Res. **3**, 25 (1971).

[68] J. M. Halbout, S. Bilt, W. Donaldson, and C. L. Tang, IEEE J. Quantum Electron. QE-15 **10**, 1176 (1979).

[69] C. J. F. Bottcher and P. Bordwyjk, *Theory of Electric Polarization* (Elsevier, Amsterdam, 1978).

[70] D. A. Kleimman, Phys. Rev. **126**, 1977 (1962).